Short pulse electron beam excitation of the high-pressure atomic Ne laser

Jong W. Shon, Robert L. Rhoades, Joseph T. Verdeyen, and Mark J. Kushner[a)]
University of Illinois, Department of Electrical and Computer Engineering, 1406 W. Green Street, Urbana, Illinois 61801

(Received 10 December 1991; accepted for publication 2 March 1993)

The high-pressure atomic Ne laser operates on four visible transitions between the $3p$ and $3s$ manifolds. Oscillation at 585 nm ($3p'[1/2]_0 \rightarrow 3s'[1/2]_1^0$) at efficiencies of $>1\%$ have been demonstrated by others. The upper laser level is believed to be populated by dissociative recombination of Ne_2^+, while state-selective Penning reactions relax the lower laser levels. To investigate these pumping mechanisms, experimental and modeling studies have been performed on a short pulse e-beam excited Ne laser using He/Ne/Ar mixtures. We found that the electron temperature in the afterglow following the e-beam pulse largely determines the time at which oscillation starts. The electron temperature during the afterglow is partly controlled by a slow relaxation of excited states in Ar. Laser oscillation does not occur until these manifolds are depleted and the electron temperature decreases, thereby increasing the rate of dissociative recombination.

I. INTRODUCTION

The high-pressure atomic neon laser operates on four transitions between the $3p$ and $3s$ manifolds (585.3, 659.9, 703.2, and 724.5 nm).[1–18] In particular, the $3p'[1/2]_0 \rightarrow 3s'[1/2]_1^0$ transition at 585 nm has attracted considerable attention in recent years as a source of efficient quasicontinuous optical power using electron beam,[2–7,10,14,15] electric discharge,[1,8,11,12,16,17] microwave,[9] and fission fragment[13] excitation.

Oscillation at 585 nm was first obtained by Bridges and Chester in 1965.[18] Little further work was reported until 1981 when Schmieder *et al.*[1] investigated electric discharge excitation at 0.7 atm using a $Ne/H_2 = 1/(0.6–1.5)$ gas mixture. They proposed that laser oscillation is made possible by quenching of the lower laser level by a Penning reaction of $Ne(3s)$ with H_2. In studies by Aleksandrov *et al.*,[5] Basov *et al.*,[3] and Bunkin *et al.*,[4] the 585 nm transition was pumped in multiatmosphere He/Ne/(Ar,Kr) gas mixtures using low-power electron beams ($10s–100s$ W cm^{-3}). They obtained laser efficiencies of 1%–1.6%. Those works, and subsequent modeling studies,[10,15] proposed that the upper laser level is populated by dissociative recombination of Ne_2^+, and that the lower laser level is depopulated by Penning ionization of the lower ionization gas additive (Ar or Kr). Aleksandrov *et al.*[5] estimated that nearly 40% of Ne_2^+ recombinations directly populate $Ne(3p'[1/2]_0)$ at high pressure (>1 atm) due to a rapid collisional relaxation of the dimer ion to its lowest vibrational state. This allows for selective population of the upper laser level by restricting the energetically permitted exit channels.

Using e-beam excitation, Basov *et al.*[3] obtained high efficiencies in, for example, $He/Ne/Ar = 50/5/1$ gas mixtures at 1–3 atm and 70 W cm^{-3}. They suggested that a possible reaction sequence leading to population of the laser level and relaxation of the lower level is[2]

$$e_{beam} + He \rightarrow He^+ \xrightarrow{He} He_2^+ \xrightarrow{Ne} Ne^+ \xrightarrow{He} HeNe^+ \xrightarrow{Ne} Ne_2^+ \xrightarrow{e} Ne(3p) \xrightarrow{h\nu} Ne(3s) \xrightarrow{Ar} Ne(2s).$$

Operating with Ne fractions higher than the optimum results in self-quenching of the laser levels by forming neon dimers from $Ne(3p)$ or directly quenching $Ne(3p) \rightarrow Ne(3s)$. Operating with Ar fractions higher than the optimum results in intercepting the formation of Ne_2^+ by charge exchange reactions of Ar with He_2^+. The dissociative recombination of Ne_2^+, which excites the upper laser level, can also be intercepted by charge exchange to Ar. Basov *et al.*[5] found that operating at higher power depositions, at least on a quasicontinuous basis, decreased and terminated laser oscillation. This was presumably due to electron collision quenching of $Ne(3p)$ and collisional radiative recombination of He_2^+.

Part of the appeal of the Ne laser for low-power electron beam and fission fragment excitation is the fact that the upper laser level is probably populated by dissociative recombination of Ne_2^+. This process has a rate coefficient that increases with decreasing electron temperature ($k \sim T_e^{-1/2}$). These excitation sources typically have lower electron temperatures (0.5–1 eV) compared to, for example, high-power discharge excited lasers. Particle beam excitation at low-power deposition produces a lower electron temperature than during high-power excitation. This is a result of recombination heating which occurs at high plasma densities.[19] Electron collision quenching of the laser levels is also minimized at low-power deposition. The moderate stopping power of He/Ne/Ar mixtures makes them particularly attractive for fission fragment excitation since high gas pressures may be used.

To investigate the sensitivity of laser oscillation to electron temperature and electron collision quenching, the Ne 585 nm high-pressure laser was experimentally investigated using short pulse e-beam excitation, and was theoretically investigated using a computer model. We found that laser oscillation occurred only after a delay following

[a)]Author to whom correspondence should be addressed.

 0021-8979/93/128059-07$06.00

the termination of the *e*-beam current pulse. This delay is inversely proportional to the amount of added He in a He/Ne/Ar mixture. Results from our computer model showed that the onset of lasing correlated with a decrease in electron temperature, which occurred when the excited state manifolds of Ar were depleted. The decrease in T_e increased the rate of dissociative recombination and pumping of the upper level.

In Sec. II, the experimental apparatus will be briefly described. The model will be described in Sec. III, followed by a discussion of our results in Sec. IV. Our concluding remarks are in Sec. V.

II. DESCRIPTION OF THE EXPERIMENT

The Ne laser using He/Ne/Ar mixtures was excited using a short pulse *e* beam. The experimental apparatus was a coaxial diode electron beam (Febetron 706).[20] The anode consisted of a 20 cm×0.6 cm (diameter) aluminum tube etched to a thickness of ≈ 130 μm. The anode also served as the pressure vessel between the laser gas mixture and the vacuum diode region, and so defined the plasma excitation region. The Febetron 706 is capable of delivering about 12 J of energy in a 600 kV pulse with a duration of 3 ns (FWHM) into a matched load. Since the diode is somewhat mismatched to the pulse forming network, the *e*-beam pulse is somewhat lengthened (4–5 ns), but is short compared to other time scales.

The distance between the mirrors of the laser cavity was 42 cm and the mirror reflectivities were 0.95 and 0.98. The experiments reported here were performed using He/Ne/Ar gas mixtures at 1–4 atm total pressure. The power deposition was estimated at 40 MW cm^{-3} at 3.72 atm. Laser power was measured with a Hammatsu R1193U-03 biplanar photodiode. All data were collected using a digital oscilloscope (Hewlett Packard 54111D).

III. DESCRIPTION OF THE MODEL

The Ne laser model consists of a full accounting of the electron and heavy particle kinetics of He/Ne/Ar mixtures. It is conceptually similar to previous models of excimer lasers[21] and of the xenon laser previously discussed by the authors.[22] The model differs from previously published models of the Ne laser by Aleksandrov *et al.*[15] and Derzhiev *et al.*[10] by including additional species to resolve intramanifold kinetics, and in details of our kinetic mechanisms.

In our model we include 33 ground state, excited, and ionic species, which encompass all levels of the Ne($3p$), Ne($3p'$), Ne($3s'$), and Ne($3s$) manifolds. In this manner, all four laser transitions can be resolved. Approximately 450 individual collisional and radiative processes are included in the model. A complete listing of the reactions and rate coefficients used in the model can be obtained by contacting the authors. W values for the *e*-beam excitation were computed using a separate Monte Carlo simulation for *e*-beam slowing for the particular gas mixtures of interest.[19] The results of the Monte Carlo simulation are also used to determine the stopping power of the gas mixture, and to properly scale the power deposition as the gas mixture is changed.

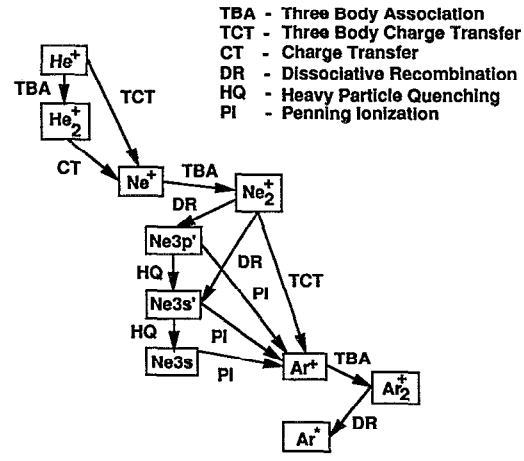

FIG. 1. Schematic of the excitation pathways of the high-pressure Ne laser. Oscillation at 585 nm occurs between Ne($3p'[1/2]_0$) and Ne($2s'[1/2]_1^0$). Excitation of the upper laser level occurs dominantly by dissociative recombination of Ne_2^+. Quenching of the lower laser level is dominantly by Penning ionization of Ar.

In the kinetics model, energy conservation equations for both heavy and light particles are used to resolve the gas and electron temperatures. The energy balance equations for the electron temperature are essentially the same as used by Kannari *et al.*[21] in which all pertinent elastic, inelastic, and superelastic collisions contribute to the electron power balance, as well as energetic contributions from slowing of beam electrons. We found that even though excited states of Ar do not directly play an important role in the excitation and relaxation kinetics of the laser levels, they are important to the electron energy balance. Therefore, a five-level model is used for the argon excited state manifolds, and coupled into the electron temperature kinetics.

Although the immediate excitation mechanism for the upper laser level is thought to be understood (dissociative recombination of Ne_2^+), the branching ratios to the upper laser and other levels, as well as the rates of quenching of those levels are not well known. (The major kinetic pathways are illustrated in Fig. 1.) We used parametric experimental data for threshold lasing and spontaneous emission from Ne($3p'[1/2]_0$) as a function of gas pressure and mixture to derive kinetically consistent values for many of these branching ratios. For example, laser oscillation only occurs after a delay of 10s to 100s ns following the current pulse, and decreases with increasing He fraction. Branching ratios for dimer recombination to individual Ne($3p'$) levels were obtained by comparing the predicted time to threshold with experiments for a series of gas mixtures. Although these branching ratios depend somewhat on our reaction scheme and are therefore not unique, we believe that they capture the essential physics.

The direct contribution of energetic beam electrons to excitation of the upper laser level was obtained by compar-

ing the model results to spontaneous emission from $Ne(3p'[1/2]_0)$. We determined that the direct and cascade contribution to $Ne(3p'[1/2]_0)$ during the *e*-beam pulse is small, even when including the effects of electron collision quenching (see Sec. IV). The fractional contribution resulting from direct *e*-beam excitation for the upper laser level, as represented by the W value for excitation during the current pulse, was determined to be less than 5%.

Although the stopping power of He is low in electron beam excitation, He^+ can be produced in large proportions when He is the dominant gas component. For example, in a He/Ne/Ar=75/15/10 mixture, approximately 30% of the *e*-beam power is directly dissipated by ionization of He. He^+, however, rapidly undergoes charge transfer reactions to He_2^+ and to Ne^+, the latter process occurring with a rate coefficient of 1.4×10^{-10} $cm^3\,s^{-1}$.[23] He^+ is therefore not directly important to the reaction scheme. As the density of Ne^+ increases during the afterglow of the *e*-beam current pulse, the dimer Ne_2^+ is formed in large quantities through three body association reactions with both Ne^+ and two body reactions with $HeNe^+$. The rate constants for the three body association reactions we used are 4.4×10^{-32} $cm^6\,s^{-1}$ for stabilization by Ne and 3.0×10^{-31} $cm^6\,s^{-1}$ for stabilization by He.[24,25] Dissociative recombination of Ne_2^+ and subsequent excitation of the upper laser level proceeds with a rate coefficient of $3.7\times10^{-8}/T_e^{-0.43}$ $cm^3\,s^{-1}$ where T_e is the electron temperature in eV.[26] The branching ratios for dissociative recombination of Ne_2^+ to the laser levels, derived in the manner described above are 40% for Ne $(3p'[1/2]_0)$, 13.8% for Ne $(3p'[1/2]_1)$ and 10% for Ne $(3s'[1/2]_1)$.

Ne_2^+ will also charge exchange to Ar^+ and Ar_2^+ by 2 body ($k=3.0\times10^{-11}$ $cm^3\,s^{-1}$) and three-body processes ($k=3.5\times10^{-30}$ $cm^6\,s^{-1}$).[26] Therefore, formation of upper laser level by dissociative recombination competes with charge transfer and dissociative recombination to Ar. When the fraction of Ar increases so that [Ar]/[*e*] exceeds $\approx2\times10^3$, the rate of charge transfer reactions from Ne_2^+ to Ar^+ exceeds the rate of dissociative recombination. This, in turn, decreases the gain. The lower laser level is dominantly quenched by Penning ionization of argon and heavy particle quenching. The rate constant we used for Penning ionization of Ar is 1.5×10^{-10} $cm^3\,s^{-1}$,[4] while the rate constant for Ar quenching of the lower laser level [$Ne(3s')+Ar\rightarrow Ne(3s)+Ar$] was estimated to be $\approx2.0\times10^{-11}$ $cm^3\,s^{-1}$.[26]

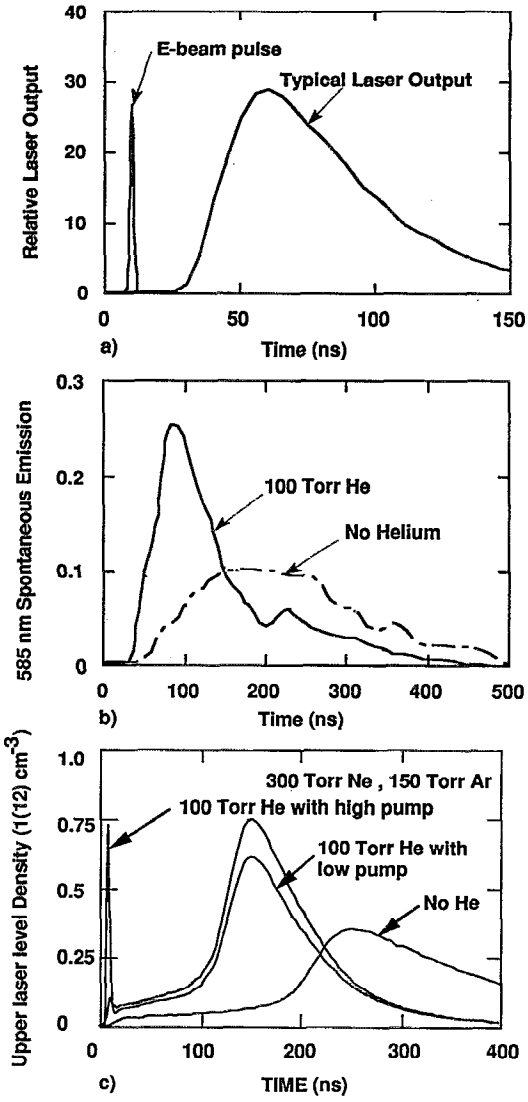

FIG. 2. Typical experimental and theoretical results for Ne laser operation. (a) Experimental results for the *e*-beam current pulse and laser oscillation at 585 nm showing the delay between the *e*-beam current pulse and onset of oscillation (He/Ne/Ar=0.7/0.2/0.1, 1.9 atm). (b) Experimental observations of spontaneous emission at 585 nm when including He (He/Ne/Ar=0.18/0.55/0.27, 550 Torr) and excluding He (He/Ne/Ar=0/0.67/0.33, 450 Torr) showing an increase in spontaneous emission with added He. (c) Theoretical results for the density of the laser level (proportional to spontaneous emission) for the experimental conditions. We also show results when a larger proportion of excitation during the *e*-beam pulse is allocated to the upper laser level. The predicted spontaneous emission during the current pulse with the larger allocation is greater than that which is experimentally observed.

IV. Ne LASER CHARACTERISTICS USING SHORT PULSE *E*-BEAM EXCITATION

Typical traces of the *e*-beam current pulse and laser emission are shown in Fig. 2(a). The *e*-beam current pulse is indicated by the x-ray flash recorded by the photodiode, somewhat broadened by detector response. The gas mixture is He/Ne/Ar=0.7/0.2/0.1 at a total gas pressure of 1.9 atm. Laser oscillation is not observed until $\approx$30 ns after the termination of the current pulse. This behavior is partly explained by the observations of spontaneous emission shown in Fig. 2(b) for He/Ne/Ar mixtures of 0.18/0.55/0.27 and 0.0/0.67/0.33. Little spontaneous emission is observed during the current pulse, suggesting that the upper laser level is not directly excited by the energetic beam electrons, or electron collision quenching during the current pulse is at least as rapid as the excitation. Adding He to the mixture shortens the delay in the spontaneous emission after the current pulse but emission still does not occur during the current pulse. Results from our model for the density of the upper laser level (proportional to spontaneous emission), which reproduce the experiment are shown in Fig. 2(c). This behavior suggests that the more rapid cooling of the electrons during the afterglow afforded

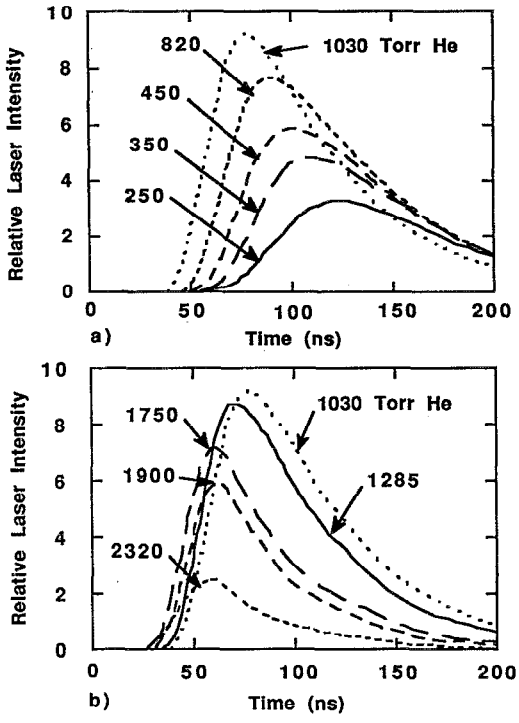

FIG. 3. Experimental results for laser intensity as a function of time for various He pressures. (a) 500–1000 Torr and (b) 1000–1900 Torr. The Ne and Ar pressures are 200 and 50 Torr, respectively. The delay between the current pulse and laser oscillation increases with increasing He pressure because the electron cooling rate increases. The laser intensity decreases at high helium pressure due to broadening of the laser transition.

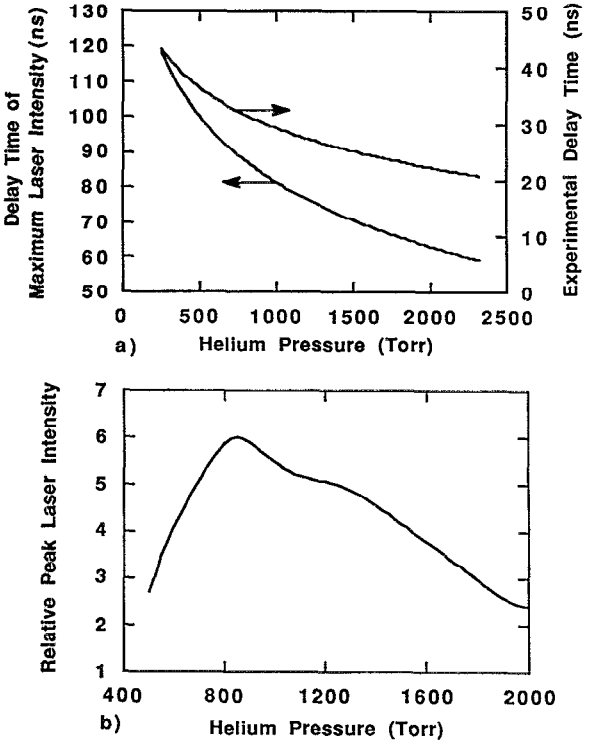

FIG. 4. Experimental results for laser parameters as a function of He pressure. (a) The delay between the current pulse, and turn on of the laser and peak intensity. (b) Maximum laser intensity. The conditions are the same as in Fig. 3.

by the added He increases the rate of dissociative recombination of Ne_2^+, which directly pumps the upper laser level.

Results from the model show that if there is any significant excitation of the upper laser level during the current pulse there should also be a substantial amount of spontaneous emission relative to the afterglow. Following these arguments, the experimental results imply that direct excitation of the laser levels during the current pulse is not particularly important. To investigate this issue, we varied the fraction of the direct excitation of neon during the current pulse that is allocated to Ne ($3p'[1/2]_0$). For example, predictions are shown in Fig. 2(c) for spontaneous emission where 0.25 of direct excitation of neon goes to the upper laser level. This produces an excessive amount of spontaneous emission, relative to that during the afterglow, compared to that observed experimentally.

Experimental laser powers as a function of time for a He/Ne/Ar gas mixture (Ne=200 Torr, Ar=50 Torr) are shown in Figs. 3(a) and 3(b) for different partial pressures of He (500–2830 Torr) yielding a total pressure of 1–4 atm. Due to the moderate stopping power of He, the total power deposition changes by only 10% over this range of gas pressures. For example, for He/Ne/Ar=500/200/50 (Torr), the power deposition is 36.2 MW cm^{-3}; at He/Ne/Ar=2830/200/50 (Torr), the power deposition is 40 MW cm^{-3}. As the amount of added helium increases up to 1500 Torr the delay time to oscillation, as well as the time at which peak laser power is obtained, decrease as shown in Fig. 4(a). The maximum laser power increases up to 1100 Torr added helium, decreasing at higher He addition [see Fig. 4(b)]. The results suggest that as the helium fraction is increased, the rate of cooling of the electrons increases due to the favorable rate of energy transfer to the light He. Since the rate of dissociative recombination of Ne_2^+, which pumps the upper laser level, increases with decreasing electron temperature, the upper laser level is being pumped at successively shorter delays with increasing He addition. As He is added to the gas mixture, the laser transition is broadened by collisions with He. Once the minimum delay is reached, this additional broadening with increasing He decreases the gain. For constant output coupling from the cavity, this decreases laser power. Since absorption at the laser wavelength is minimal, some portion of the reduced performance could be recouped by optimizing the cavity parameters to match the lower gain.

Results from our model for laser intensity as a function of gas mixture for the experimental conditions of Fig. 3 are shown in Fig. 5(a). The predicted delay time to laser oscillation and peak intensity, and the relative peak intensities are shown in Fig. 5(b). We also obtain a decrease in the delay time to threshold with increasing He addition which, with a fixed offset, agrees well with the experiment. The decrease in delay is largely due to the increasing rate of electron cooling with added He, discussed in more detail below.

The contribution of broadening of the laser transition

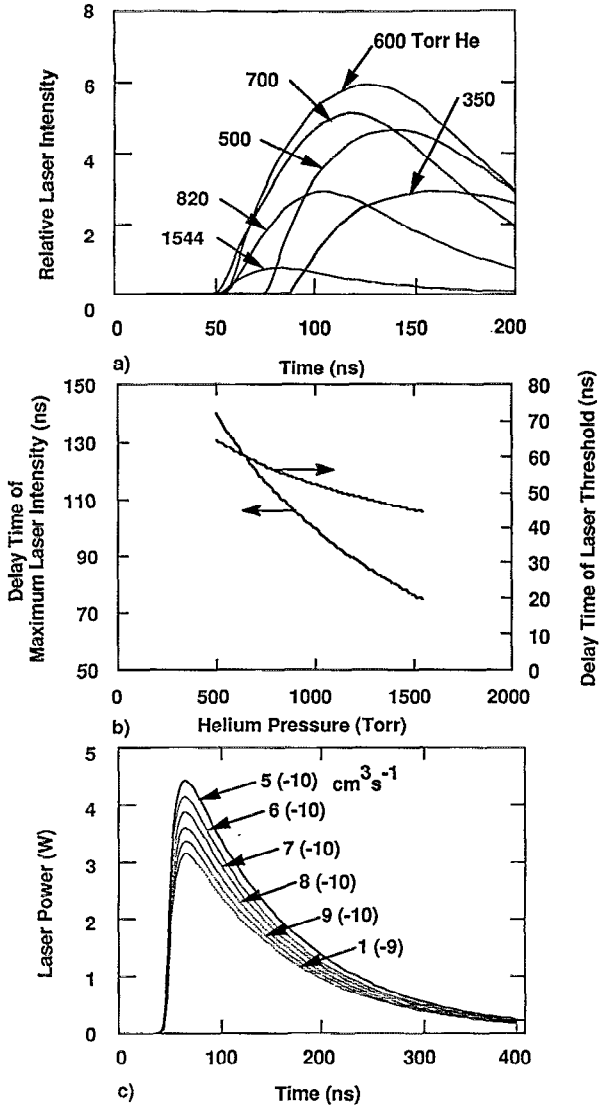

FIG. 5. Results from the model for (a) laser intensity as a function of time for various He partial pressures (b) delay in onset of laser oscillation and peak intensity and (c) laser intensity as a function of the broadening coefficient for the laser transition. The gas pressure is 3.6 atm while the other conditions are the same as for the experimental results in Fig. 3. The decrease in delay time can be attributed to a higher rate of electron thermalization. The decrease in laser intensity can be attributed to broadening.

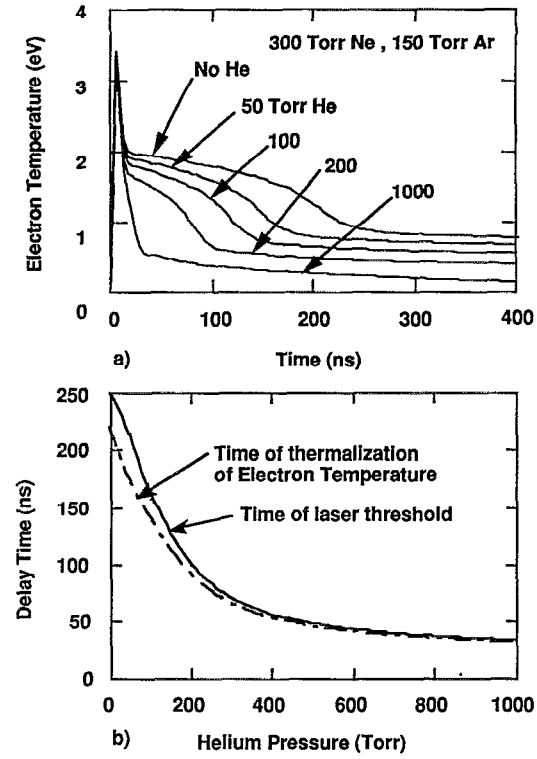

FIG. 6. Predictions from the model for (a) electron temperature as a function of time for various partial pressures of He, and (b) times at which the electron distribution thermalizes and the time at which oscillation starts. The gas mixture is Ne=300 Torr, Ar=200 Torr with the indicated amounts of He. The electron temperature quickly falls to a plateau value after the *e*-beam current pulse. Laser oscillation does not occur until the electron temperature falls off this plateau.

to the decrease in laser power was investigated with the model. Aleksandrov *et al.*[15] measured the broadening coefficient of the 585 nm transition by collisions with He and obtained $\gamma=0.62\times10^{-9}$ cm^3 s^{-1}. We parametrized this broadening coefficient in the model between 0.5×10^{-10} and 1×10^{-9} cm^3 s^{-1}, and the predicted laser powers are shown in Fig. 5(c) for He/Ne/Ar=0.7/0.2/0.1 at 3.6 atm. An increase in broadening does not appreciably change the delay time to threshold, since this value is largely determined by the onset of dissociative recombination resulting from the cooling of the electrons. Once threshold is reached, however, the broadening of the transition increases the saturation intensity. This allows other parasitic processes such as electron collision quenching to lower the inversion density and hence laser power.

Predicted electron temperatures as a function of time for gas mixtures containing Ne=300 Torr and Ar=150 Torr are shown in Fig. 6(a) for various He pressures. During the *e*-beam current pulse the electron temperature reaches a maximum value of $\approx$3 eV. Immediately after the *e*-beam current pulse, the electron temperature cools to a plateau value of 0.5–1.0 eV. The plateau value decreases with increasing He fraction, a consequence of the more rapid rate of electron cooling afforded by more efficient energy exchange collisions with He. This plateau value is sustained for 10*s*–100*s* ns, at which time the electron temperature again falls to a value of 0.05–0.2 eV, and continues to slowly thermalize to the gas temperature. The onset of laser oscillation coincides with the fall in electron temperature from its plateau value. This correlation is shown in Fig. 6(b) where the time of the onset of laser oscillation and the time at which the electron temperature falls off the plateau are plotted.

The plateau value of the electron temperature is sustained by heating from superelastic electron collisions with excited state manifolds. Since excitation transfer results in a rapid cascade of population from He to Ne, and ultimately to Ar, the majority of the superelastic collisions

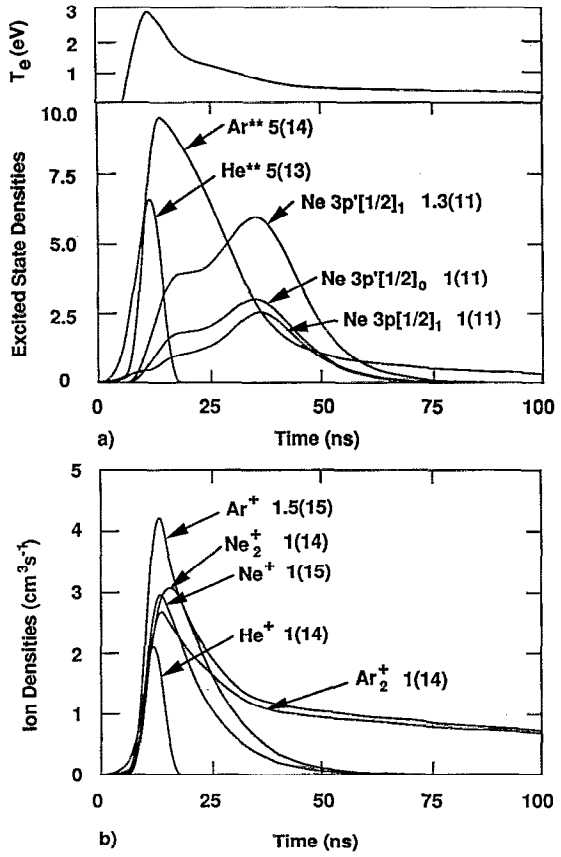

FIG. 7. Selected species densities (cm^{-3}) predicted by the model, (a) neutral states and (b) ions. The time dependence of the electron temperature is shown at the top of the figure. The gas mixture is He/Ne/Ar =0.7/0.2/0.1. The densities of excited states of argon are much greater than He and Ar. The electron distribution does not cool until these states are depleted by superelastic collisions. The normalizing factors for each species density are shown in the figure.

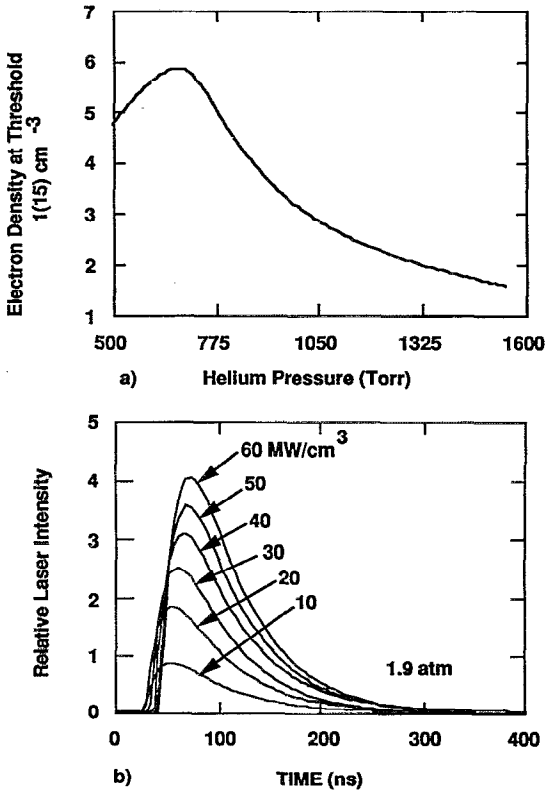

FIG. 8. Predicted laser parameters; (a) electron density at the onset of lasing as a function of He partial pressure. The gas mixture is Ne (200 Torr) and Ar (50 Torr) with the indicated amount of He. (b) Laser intensity as a function of pump rate for a He/Ne/Ar=0.7/0.2/0.1 mixture at 3 atm. Unlike the xenon laser, there is no direct correlation between the onset of lasing and the electron density (or fractional ionization), thereby implying that electron collision mixing is not particularly important. This is confirmed by the nearly linear increase in laser intensity with pump rate.

that heat the electrons during the plateau period are with excited states of Ar. The correlation between electron temperature and excited state densities is shown in Fig. 7(a). Here the densities of excited states of He, Ne, and Ar, and the electron temperature are plotted as a function of time for a He/Ne/Ar=0.7/0.2/0.1 mixture. Selected ion densities for the same conditions are plotted in Fig. 7(b). For these conditions, 39% of the *e*-beam energy is deposited in Ar, and 45% of the beam energy is deposited in He. Excitation transfer from He to Ne and Ar, and from Ne to Ar occurs rapidly until the densities of excited states of Ar greatly exceed those of excited states of He and Ne. Ar is also the most plentiful ion. The excited states of Ar therefore dominate the energy exchange with electrons during the afterglow. When excited states of Ar are depleted by superelastic collisions, the source of electron heating is exhausted, and the electron temperature is allowed to decrease. At this time, the rate of dissociative recombination increases with the fall of the electron temperature, and excited states of Ne are rapidly populated. The density of Ar_2^+ remains high throughout this period because Penning processes of Ne ($3s$) with Ar continue to generate Ar^+.

It has been proposed that electron collision mixing (ECM) of the laser levels of the atomic xenon ($5d \rightarrow 6p$) laser is a limiting process, and restricts operation of the xenon laser to a fractional ionization of $<10^{-5}$. In experiments performed by Peters *et al.*,[27] a delay in the onset of oscillation of a xenon laser excited by a short pulse *e*-beam was observed. This behavior was attributed to the time that was required for the electron density to decrease below a critical value above which ECM prevented oscillation. We investigated whether ECM is a limiting process in the Ne laser. The electron density at the time at which laser oscillation begins in the Ne laser, as predicted by the model, is plotted in Fig. 8(a). The gas mixture is 200 Torr of Ne, 50 Torr of Ar, and the noted balance of He. The rate coefficient used for superelastic relaxation of Ne($3p'[1/2]_0$) is 8.8×10^{-9} cm^{-3} s^{-1}. Endothermic rates are given by detailed balance. There is not a strong correlation between the onset of oscillation and the electron density or fractional ionization. This suggests that ECM is less a factor in the Ne laser (at these excitation levels) compared to the xenon laser. This behavior was confirmed by varying the pump rate in the model. Laser powers as function of pump rate are shown in Fig. 8(b) for a He/Ne/Ar mixture at 3

atm. The laser power is nearly proportional to the pump rates above threshold. The laser turns on slightly earlier at the lower pump rates due to the smaller amount of ECM. The onset of the laser oscillation, though, is only a weak function of pump power compared to its dependence on He partial pressure.

Quasicontinuous operation of the Ne laser by others has shown that the optimum laser efficiency occurs with a Ne/Ar ratio of approximately 2/1. We parametrized the Ne/Ar ratio in the model. We found that laser power as a function of Ar pressure optimizes at a Ne/Ar ratio of 4/1. Laser oscillation does not occur until an Ar pressure of $\approx$20 Torr. The experimental threshold for laser oscillation is $\approx$15 Torr of Ar. At low Ar pressures, there is not sufficient quenching of the lower laser level. At high Ar pressures, Ne_2^+ is intercepted prior to undergoing dissociative recombination.

V. CONCLUDING REMARKS

The kinetics of the Ne 585 nm high-pressure laser using He/Ne/Ar mixtures have been experimentally and theoretically investigated using short pulse *e*-beam excitation. The experimental results are well explained by the upper laser level being dominantly excited by dissociative recombination of Ne_2^+ during the afterglow following the current pulse. The onset of laser oscillation occurs when the electron temperature falls to a few tenths of an eV and the rate of dissociative recombination increases. The lower laser level is largely quenched by Penning ionization with Ar. We found that details of the Ar kinetics are important since superelastic heating of the electrons from excited states of Ar maintains the temperature at a sufficiently high value to prevent laser oscillation. During quasicontinuous operation of the Ne laser, a higher electron temperature is compensated by a higher plasma density, which increases the rate of recombination and pumping of the upper laser level.

ACKNOWLEDGMENTS

The authors wish to thank G. Hebner and G. Hays for their advice on Ne laser kinetics. This work was supported by Sandia National Laboratory and by the National Science Foundation (ECS91-09326, CTS91-13215).

[1] D. Schmieder, D. J. Brink, T. I. Salamon, and E. G. Jones, Opt. Commun. **36**, 223 (1981).
[2] N. G. Basov, A. Yu. Aleksandrov, V. A. Danilychev, V. A. Dolgikh, O. M. Kerimov, Yu. F. Myznikov, I. G. Rudoi, and A. M. Soroka, Sov. Tech. Phys. Lett. **11**, 181 (1985).
[3] N. G. Basov, A. Yu. Aleksandrov, V. A. Danilychev, V. A. Dolgikh, O. M. Kerimov, Yu. F. Myznikov, I. G. Rudoi, and A. M. Soroka, JETP Lett. **41**, 192 (1985).
[4] F. V. Bunkin, V. I. Derzhiev, G. A. Mesyats, V. S. Skakun, V. F. Tarasenko, and S. I. Yakovlenko, Sov. J. Quantum Electron. **15**, 159 (1985).
[5] A. Yu. Aleksandrov, V. Yu. Anan'ev, N. G. Basov, V. A. Danilychev, V. A. Dolgikh, A. A. Ionin, O. M. Kermiov, A. P. Lytkin, Yu. F. Myznikov, I. G. Rudoi, and A. M. Soroka, Sov. Phys. Dokl. **30**, 875 (1985).
[6] A. Yu. Aleksandrov, V. A. Dolgikh, O. M. Kermiov, A. P. Lytkin, Yu. F. Myznikov, G. Rudoi, and A. M. Soroka, Sov. J. Quantum Electron. **17**, 1521 (1987).
[7] A. Yu. Alekandrov, V. A. Dolgikh, G. Rudoi, and A. M. Soroka, Sov. J. Quantum Electron. **18**, 965 (1988).
[8] I. I. Murav'ev, E. V. Chernikova, and A. M. Yancharina, Sov. J. Quantum Electron. **19**, 123 (1989).
[9] V. A. Vaulin, V. I. Derzhiev, V. M. Lapin, V. N. Slinko, S. S. Sulakshin, S. I. Yakovlenko, and A. M. Yancharina, Sov. J. Quantum Electron. **19**, 323 (1989).
[10] V. I. Derzhiev, A. G. Zhidkov, A. V. Koval, and S. I. Yakovlenko, Sov. J. Quantum Electron. **19**, 1016 (1989).
[11] T. M. Gorbunova, V. I. Derzhiev, Y. P. Mikhailchenko, E. V. Chernikova, S. I. Yakovlenko, and A. M. Yancharina, Sov. J. Quantum Electron. **20**, 1191 (1990).
[12] E. L. Latush, M. F. Sem, and G. D. Chebotarev, Sov. J. Quantum Electron. **20**, 1327 (1990).
[13] G. A. Hebner and G. N. Hays, Appl. Phys. Lett. **57**, 2175 (1990).
[14] A. Y. Aleksandrov, V. A. Dolgikh, I. G. Rudoi, and A. M. Soroka, Sov. J. Quantum Electron. **21**, 611 (1991).
[15] A. Y. Aleksandrov, V. A. Dolgikh, I. G. Rudoi, and A. M. Soroka, Sov. J. Quantum Electron. **21**, 933 (1991).
[16] P. M. Pramatarov, M. S. Stefonva, M. Ganciu, A. V. Karelin, A. M. Yancharina, J. P. Ivanova, and S. I. Yakovlenko, Appl. Phys. B **53**, 30 (1991).
[17] M. Ganciu, A. Surmeian, C. Diplasu, I. Chera, G. Musa, and I. -Iovitz Popescu, Opt. Commun. **88**, 381 (1992).
[18] W. B. Bridges and A. N. Chester, Appl. Opt. **4**, 573 (1965).
[19] M. J. Kushner, J. Appl. Phys. **66**, 2297 (1989).
[20] R. L. Rhoades and J. T. Verdeyen, Appl. Phys. Lett. **60**, 2951 (1992).
[21] F. Kannari, W. D. Kimura, and J. J. Ewing, J. Appl. Phys. **68**, 2615 (1990).
[22] M. Ohwa, T. J. Moratz, and M. J. Kushner, J. Appl. Phys. **66**, 5131 (1989).
[23] D. L. Albritton, At. Data Nucl. Tables **22**, 1 (1978).
[24] R. Johnsen and M. A. Biondi, J. Chem. Phys. **73**, 5045 (1980).
[25] G. E. Veach and H. J. Oskam, Phy. Rev. A **2**, 1422 (1970).
[26] L. A. Levin, S. E. Moody, E. L. Klostermann, R. E. Center, and J. J. Ewing, J. Quantum Electron. **QE-17**, 2282 (1981).
[27] P. J. Peters, Y. F. Lan, M. Ohwa, and M. J. Kushner, IEEE J. Quantum Electron. **QE-26**, 1964 (1990).